

Electron stimulated desorption from CaF_2 : penetration depth of electrons and sample charging

R. Bennewitz^a, D. Smith^a, M. Reichling^{a,*}, E. Matthias^a, N. Itoh^b, R.M. Wilson^c

^a *Fachbereich Physik, Freie Universität Berlin, Arnimallee 14, 14195 Berlin, Germany*

^b *Department of Physics, Nagoya University, Furo-Cho, Chikusa, Nagoya 464-01, Japan*

^c *Department of Physics, Wake Forest University, Winston-Salem, NC 27109, USA*

Abstract

Two aspects of electron stimulated desorption experiments are covered in this contribution, namely the energy deposition of low energy electrons in CaF_2 and the charging of the surface during irradiation. The stopping power for electron energies in the range from 50 eV to 5 keV is calculated using optical absorption data. Energy deposition curves and penetration depth vs. electron energy curves are given based on stopping power values and a Monte Carlo simulation of elastic scattering. Charging of the surface is described by means of an equilibrium between primary and secondary electrons. The sensitivity of the surface charging to stoichiometric changes is shown by monitoring the kinetic energy of desorbing F^+ ions during metallization of the surface.

1. Introduction

Electron stimulated desorption (ESD) of alkali halides has been studied extensively for several decades [1]. However, there are only few studies of ESD from CaF_2 [2, 3]. We have studied desorption of ions and neutrals from CaF_2 irradiated with 1 keV electrons and believe that the desorption of F^+ ions in a Knotek–Feibelman process to be one of the dominant processes [4]. The present contribution deals with two important aspects of ESD experiments on CaF_2 , namely the stopping power for primary electrons in CaF_2 determining the depth of energy deposition in the crystal and charging of the sample during irradiation that influences the emitted ions.

2. Stopping power for low energy electrons

Fundamental to many DIET measurement interpretations is the premise that desorption events are diffusion limited. That is, the role of defect diffusion largely determines how sputtering efficiency and surface metallization vary with incident electron energy. Accordingly, models of electron–crystal interaction must describe the effective penetration depth of electrons with variations of beam

energy and the form of energy loss in a solid. As a way of understanding electron interactions for the case of alkaline-earth halides, and extending the extrapolation validity to low energy, we have calculated the stopping power of CaF_2 for low energy electrons using optical constants listed in [5]. The calculation method is based on a model suggested by Ashley [6], which assumes a simple quadratic rule between the energy and momentum in order to extend the imaginary part of the optical dielectric function with zero momentum transfer to the dielectric function with finite momentum transfer. The optical data obtained for a limited energy range (typically below 40 eV) have been extrapolated using the power relation for the optical reflectivity $k\omega^{-4}$, where k is a constant and $h\omega/2\pi$ the photon energy. The Kramer–Kronig relation is used to obtain the imaginary part of the optical dielectric function over a wide energy range [7]. The validity of the extrapolation has been tested using the f-sum rule.

The obtained values for the stopping power are shown in Fig. 1. For the case of 1 keV electrons the stopping power has a maximum at an energy of approximately 200 eV close to $5 \text{ eV}/\text{\AA}$. These results can be used to calculate the mean energy deposited in the first triple layer (F–Ca–F) of the (111) surface by multiplying the stopping power for 1 keV electrons with the thickness of the layer: 10.5 eV per incident electron. Therefore, the effectiveness of creating an electron–hole pair in the first layer is about 0.3 per incident electron assuming that the

*Corresponding author.

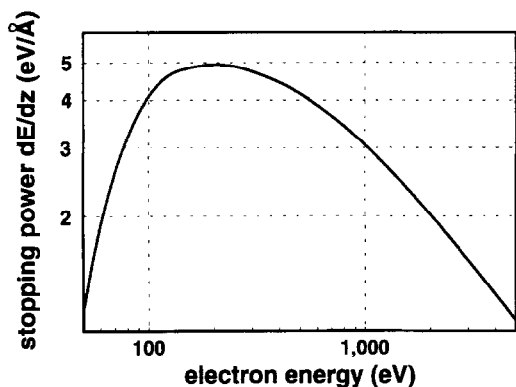


Fig. 1. Stopping power for CaF_2 calculated using the Ashley model.

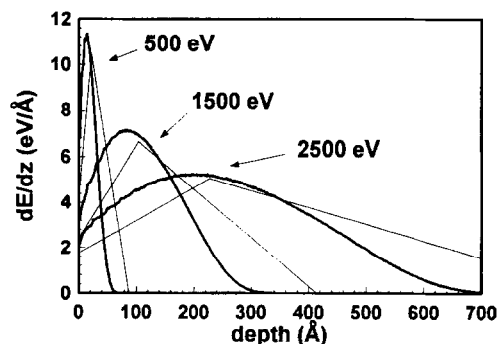


Fig. 2. Energy deposition curves based on the stopping power calculation and a Monte Carlo simulation of elastic scattering (thick lines) together with curves according to the model of Al Jammal et al. (thin lines). Incident energies are 0.5, 1.5, and 2.5 keV.

creation of the electron–hole pair needs an energy of three times the bandgap. Estimates of this kind can be helpful for the study of cross sections of different desorption processes.

The energy deposition curve dE/dz has been calculated by using the stopping power values for a continuous slowing down approach and simulating elastic scattering in a Monte Carlo code based on screened Rutherford scattering cross sections. These calculations exactly follow the method suggested by Scott and Love [8]. For purposes of comparison the results are plotted in Fig. 2 together with curves based on the well-known model of Al Jammal, Pooley, and Townsend [9]. The corners of the triangles are given by the stopping power value for the primary electron energy, by the maximum range of electrons calculated from the stopping power values neglecting elastic scattering, and by the total area below the curve which has to be set equal to the primary

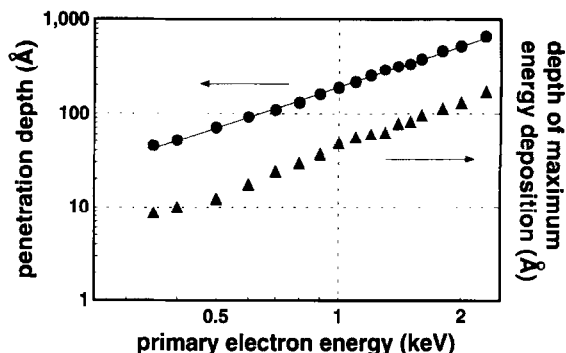


Fig. 3. Penetration depth of electrons and position of maximum energy deposition as a function of electron energy in CaF_2 .

electron energy. The peak of the triangle has been positioned at 25% of the maximum electron range.

Fig. 2 demonstrates that the simple approach of Al Jammal et al. is quite a reasonable estimate for the depth dependence of the energy deposition by low energy electrons. However, it systematically overestimates the maximum penetration depth and, therefore, yields values too low for the energy deposition near the surface.

Fig. 3 shows penetration depth as a function of electron energy as obtained from the Monte Carlo code. Fitting the curve yields a value for the electron depth as a function of energy according to $D = 190 \text{ \AA} \cdot (E/\text{keV})^{1.45}$. Additionally, the peak position of the energy deposition is given which turns out to be 25% of the maximum penetration depth, except for energies lower than 800 eV where it tends to become less than 25%.

3. Charging by electron irradiation

Charging of insulators subject to electron irradiation is a well-known phenomenon that lowers the resolution in experimental techniques like scanning electron microscopy [10] or Auger electron spectroscopy [11]. Valuable surveys on different approaches to features occurring due to low energy electron irradiation are given by Cazaux [12] and Miotello [13]. The charging of alkali and alkaline-earth halides irradiated with 1 keV electrons will be described in the following paragraph for defocusing conditions; i.e. for a beam diameter much larger than the penetration depth of the electrons.

While the bulk of the insulator is negatively charged down to the penetration depth of the electrons, the surface is positively charged due to the secondary electron emission with a coefficient $\sigma = 3.2$ secondary electrons per incident electron [14]. The surface potential U is determined by the secondary electron distribution $d\sigma/dE$: secondary electrons with an energy lower than eU are pulled back to the surface by the attractive

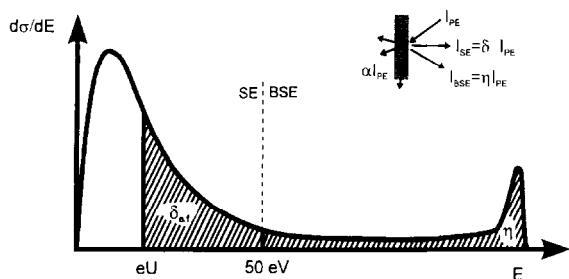


Fig. 4. Schematic energy distribution of secondary electrons. The charging yields an equilibrium if the integral over the marked area is 1. The integral over the complete distribution curve is equal to the secondary electron coefficient $\sigma = 3.2$.

potential (Fig. 4). The value of U is given by an equilibrium between primary current I_{PE} and the sum of back-scattered electrons ηI_{PE} and escaping secondary electrons $\delta_{eff} I_{PE}$. Therefore, U depends only on the secondary electron distribution but not on the current I_{PE} . The equilibrium between primary and secondary electrons can be shifted by additional currents αI_{PE} to or from the surface; e.g. the surface charging is lowered by the desorption of positive ions or by leakage currents between the irradiated spot and the grounded sample holder. Due to this indirect effect charging during ESD experiments may well be depending on I_{PE} .

Measurements of the F^+ desorption including the kinetic energy distribution of the ions have been performed using an ion energy selective mass spectrometer (HIDEN HAS 5PL) with an energy resolution of 0.5 eV. Since we believe that the F^+ ions desorb by a Knotek–Feibelman mechanism and we expect desorption energies around 1 eV, the kinetic energy can yield information about the potential difference of the irradiated surface and the grounded entrance slit of the mass spectrometer. Fig. 5 shows a typical energy distribution of F^+ ions during 1 keV irradiation. The symmetric shape of the distribution and its base width remain unchanged during irradiation for different applied current densities and temperatures. In contrast, peak height and position undergo a strict temporal evolution during continued irradiation that does depend on current density and temperature. Miura et al. [3] observed a similar energy distribution and explained the width of this distribution as originating from the desorption process. Based on the assumption that the kinetic energy of the desorbing ions comes from the excess energy of an Auger transition, they model the width as a convolution of the widths of those atomic levels involved in the Auger transition of the Knotek–Feibelman process. However, in the case of a bulk crystal the width may also be caused by the inhomogeneous distribution of charging over the finite beam radius. It is still an open question how much of the kinetic energy of the desorbing F^+ originates from the

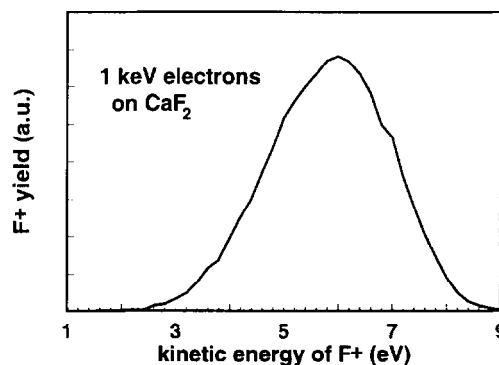


Fig. 5. Distribution of kinetic energy of F^+ ions desorbing from CaF_2 during 1 keV electron irradiation.

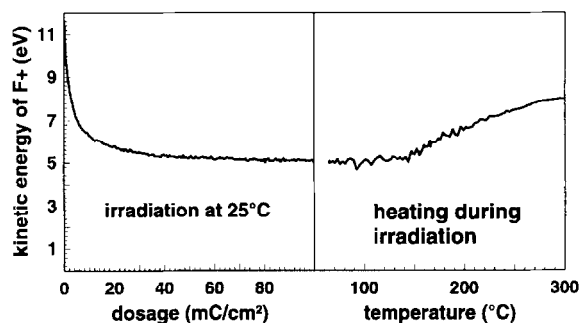


Fig. 6. Influence of irradiation damage on the surface charging monitored by the kinetic energy of desorbing F^+ ions.

desorption process and how much from the surface charging.

Since the secondary electron coefficient of metallic calcium [15] is only 0.8, an insulated piece of metallic calcium would be negatively charged by the electron beam. Therefore, the charging is very sensitive to changes of the surface stoichiometry, especially to the metallization of CaF_2 by electron irradiation. Scanning force microscopy measurements [16] have shown that such stoichiometric changes appear in form of mesoscopic colloids at the CaF_2 surface subject to electron irradiation.

The effect of metallization and crystal temperature on surface charging is demonstrated in Fig. 6. Charging is monitored by the average kinetic energy of F^+ ions desorbed during 1 keV electron irradiation. At the beginning of irradiation the charging is about 11 V decreasing rapidly and approaches a value of 5 V for constant irradiation at a fixed temperature. F^+ desorption must take place between colloids and, therefore, the observed shift in kinetic energy represents the charging changes of a damaged but not completely metallized surface, which would be expected to charge negatively. The saturation of the charging decrease is consistent with the observed

saturation of metallization due to inhibiting defect production by absorption of most electrons in metal colloids.

Heating the sample during continued irradiation yields desorption of neutral calcium starting at about 150°C. This thermal evaporation of the metal on the surface may reestablish the ordered CaF₂ surface as indicated by the rise of the charging to be seen in the right-hand part of Fig. 6. At 300°C charging has not yet reached the value of 11 V observed for the undamaged surface implying that at 300°C there is still excess metal on the surface, although, metallic calcium evaporates.

References

- [1] M. Szymonski, *Mat. Fys. Medd. Dan. Vid. Selsk.* 43 (1993) 495.
- [2] W. Husinsky, P. Wurz, K. Mader, E. Wolfrum, B. Strehl, G. Betz, R.F. Haglund, A.V. Barnes and N.H. Tolk, *Nucl. Instr. and Meth.* B33 (1988) 824.
- [3] K. Miura, K. Sugiura and H. Sugiura, *Surf. Sci. Lett.* 253 (1991) L407.
- [4] M. Reichling, these Proceedings, *Nucl. Instr. and Meth.* B101 (1995) 108.
- [5] E.D. Palik, ed., *Handbook of Optical Constants of Solids II* (Academic Press, New York, 1991).
- [6] J.C. Ashley, *J. Elec. Spectr. Rel. Phenom.* 46 (1988) 199.
- [7] M.W. Williams, D.W. Young, J.C. Ashley and E.T. Arakawa, *J. Appl. Phys.* 58 (1985) 4360.
- [8] M.G.C. Cox, in: *Quantitative Electron-Probe Microanalysis*, V.D. Scott and G. Love, eds. (Ellis Horwood Limited, Chichester, 1983).
- [9] Y. Al Jammal, D. Pooley and P.D. Townsend, *J. Phys. C: Solid State Phys.* 6 (1973) 247.
- [10] L. Reimer, *Image Formation in Low-Voltage Scanning Electron Microscopy*, (SPIE Optical Engineering Press, 1993).
- [11] D.P. Russell, W. Durrer, J. Ramirez and P.W. Wang in: *Springer Series in Surface Science, Vol. 31, DIET V*, eds. A.R. Burns, E.B. Stechel, D.R. Jennison (Springer, Berlin, Heidelberg, 1993).
- [12] J. Cazaux, *J. Appl. Phys.* 59 (1986) 1418.
- [13] A. Miotello, *J. Phys. C*19 (1986) L201–L206.
- [14] H. Bruining and J.H. de Boer, *Physica* 6 (1939) 834.
- [15] I.M. Bronshtein and B.S. Fraiman, *Sov. Phys. Sol. Stat.* 3 (1961) 995.
- [16] R. Bennewitz, M. Reichling, R.M. Wilson, R.T. Williams, K. Holldack, M. Grunze, E. Matthias, *Nucl. Instr. and Meth.* B91 (1994) 623.